

**Quarterly reports on the state of the ocean:  
Meridional heat transport variability in the Atlantic Ocean**  
Molly Baringer, Silvia Garzoli, Gustavo Goni, Carlisle Thacker and Rick Lumpkin  
NOAA Atlantic Oceanographic and Meteorological Laboratory, Miami FL

## **1. PROJECT SUMMARY**

**Goal:** To contribute to the assessment of the state of the ocean by providing quarterly reports on the meridional heat transport in the Atlantic Ocean. This heat transport is directly related to the role that this basin plays in the meridional overturning circulation (MOC) and is an important benchmark for integrated air-sea fluxes and numerical model performance.

**Project Output:** “State of the ocean” quarterly estimates of meridional oceanic heat transport in the center of the subtropical gyres in the North and South Atlantic. This project funds the development of a methodology to estimate heat transport variability using data collected along two high density XBT lines operated by AOML, satellite data (altimeter and scatterometer), wind products from the NCEP reanalysis and products from general circulation models. Quarterly reports are posted on the AOML web site.

**General Overview:** The Atlantic Ocean is the major ocean basin involved in large-scale northward transports of heat typically associated with the meridional overturning circulation (MOC) where warm upper layer water flows northwards, and is compensated for by southward flowing North Atlantic Deep Water. This large-scale circulation is responsible for the northward heat flux through the entire Atlantic Ocean. Historical estimates of the net northward heat flux in the vicinity of its maximum, which occurs in the North Atlantic roughly at the latitude of the center of the subtropical gyre, range from 0.9 PW<sup>1</sup> to 1.6 PW, while estimate in the 30°S to 35°S band are even more uncertain, ranging from negative to more than 1 PW. While much of this variability may be a consequence of the different methods used to estimate the heat transport, natural variability cannot be ruled out. The importance of this heat transport to the world climate together with the possibility of monitoring its variability motivates this project.

AOML collects XBT data on two lines spanning the subtropical oceans: in the North Atlantic since 1995 (quarterly repeats) along AX7 running between Spain and Miami, Florida and in the South Atlantic since 2002 (twice per year until 2004 and quarterly thereafter) along AX18 between Cape Town, South Africa and Buenos Aires, Argentina. These data capture the upper limb of the MOC transport. In the North Atlantic much of the northward transport is confined to a strong boundary current through the Florida Straits, where XBT data can also be usefully augmented with other data from the NOAA/OCO funded Florida Current transport program.

---

<sup>1</sup> PW is PetaWatt or 10<sup>15</sup> Watts, a unit of power commonly used for ocean heat transports.

Heat transports have already been successfully computed using XBT data (Roemmich et al, 2001), however the methodology for estimating the transport can be improved. In particular, as density is essential for the flux estimates, results depend on how well salinity profiles can be estimated to complement the XBT data and on how well the profiles can be extended to the bottom of the ocean. Improving these estimates to achieve more accurate fluxes is an essential part of this project, as is a careful quantitative assessment of the accuracy of the resulting fluxes.

**Methodology:** Northward mass, volume, and heat transport through a vertical plane can be estimated directly from observations. The northward velocity  $v$  can be treated as a sum of three terms: (i) a geostrophic contribution (thermal wind equation) relative to a prescribed reference level, (ii) an ageostrophic part modeled as Ekman flow, and (iii) a barotropic part defined as the velocity at the reference level. Density  $\rho$  can be obtained from XBT data if salinity is accurately estimated and data are extrapolated to the ocean bottom.

$$\begin{array}{lll} M = \iint \rho v \, dx dz & V = \iint v \, dx dz & H = \iint \rho c_p \theta v \, dx dz \\ \text{[Kg/s]} & \text{[Sv} = 10^6 \text{ m}^3 / \text{s]} & \text{[PW} = 10^{15} \text{ Watts]} \end{array}$$

Estimates of mass and heat transport have been obtained from temperature profiles collected along AX07 and AX18 high-density lines using Sippican T-7 XBT probes, which typically provide data to 800 m or deeper. Salinity was estimated for each profile by linearly interpolating the closest of Levitus' climatological mean salinity and temperature profiles to the XBT temperature and the climatological profiles were used to extend the data to the bottom. In computing geostrophic velocities, a reference level, based on previous work in the literature and on what is known about the circulation, was prescribed just below the northward flowing Antarctic Intermediate Water ( $\sigma_0=27.6 \text{ kg m}^{-3}$  in the North Atlantic and  $\sigma_0=27.4 \text{ kg m}^{-3}$  in the South Atlantic). Within strong flows such as the Florida Current or the Malvinas Current where no level of “no motion” can be found, the transport must be specified (e.g. by the mean value of the Florida Current, etc.). The velocity at the reference level is adjusted so that the net mass transport across the section is zero using a single velocity correction for each section. Typically, values of this correction ranged from  $10^{-4}$  to  $10^{-6} \text{ m s}^{-1}$ .

## 2. ACCOMPLISHMENTS

### 2.1. Products Delivered

Quarterly reports were designed that show the estimated heat transport for each high density XBT section along the AX7 and AX18 lines (Figure 1 and 2) and are posted quarterly on AOML's state of the ocean web site at <http://www.aoml.noaa.gov/phod/soto/mht/index.php>. Each figure shows: the position of the most recent XBT transect (red) and the position of the all the transects completed to date (blue) (Top left panel); the temperature section corresponding to the last section (top

right panel); the time series of the obtained values for the different components of the heat transport (bottom left) and the annual cycle of the heat transport components (bottom right).

Values of heat transport are given in PW ( $1 \text{ PW} = 10^{15} \text{ W}$ ). One PW is equivalent to the amount of electricity produced by *one million* of the largest nuclear power plants in existence today (the largest nuclear plants produce about 1 gigaWatt of electrical power).

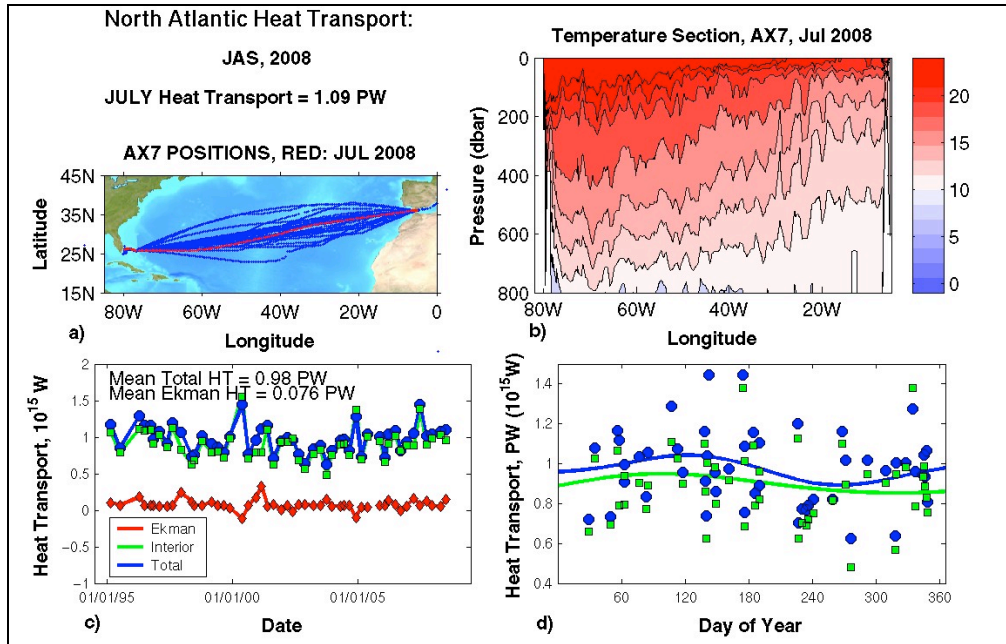


**Figure 1:** Report for the July-August-September quarter of 2007 for North Atlantic Meridional Heat transport along the AX7 high density XBT line. Transport results based on July 2008 XBT section (positions shown in top left, temperature section shown in top right). Heat transport estimates were decomposed into the geostrophic (interior) and Ekman components and their total (lower left).

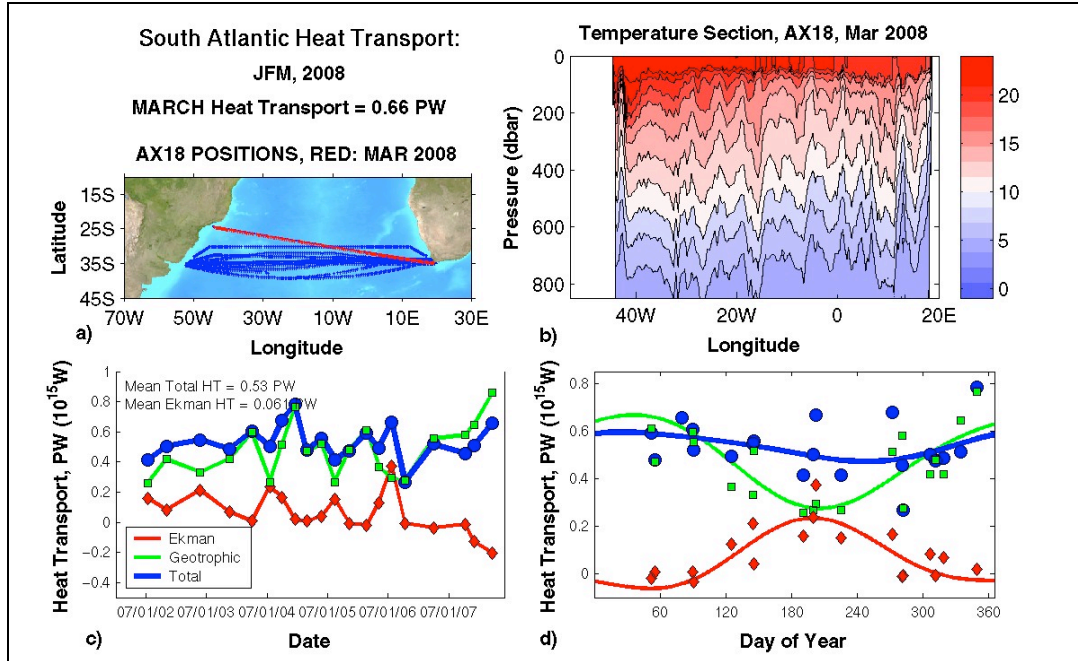


**Figure 2:** Report for the January-February-March quarter of 2008 for South Atlantic Meridional Heat transport along the AX18 high density XBT line. Transport results based on March 2007 AX18 XBT section (positions shown in top left, temperature section shown in top right). Heat transports were estimated using a shallow (green squares) and deep (red diamonds) reference level (lower left). Total heat transports demonstrate no significant seasonal signal because the seasonal signal in the Ekman layer is directly out of phase with the geostrophic signal (lower right).

## 2.2. Scientific Findings

### *South Atlantic:*

The methodology described above was applied to the South Atlantic data and an intensive study of the errors was completed (Baringer and Garzoli, 2007). Garzoli and Baringer (2007) applied this method to the fourteen high-density XBT AX18 sections collected between July 2002 and May 2006 to compute the meridional heat transport in the South Atlantic. The integrated volume transport yields a mean value for the total transport east of the Walvis ridge of 28 Sv, 19 Sv for the Brazil Current (between 0 and 800 m) and -9 Sv for the DWBC (2500 to 6000). These values are in agreement with the previous calculations obtained from direct observations. The net flow in the center of the basin ranges from 0 to 30 Sv depending on the structure of the wind. The values obtained for the heat transport ranged from 0.40 to 0.81 PW with a mean value of 0.54 PW and a standard deviation of 0.11 PW. The total heat transport does not show any significant change with time (Figure 4). The variability in heat transport may be a consequence of the natural physics of the system or may be related to the difference in cruise track (sampling different physical regimes). The variability of the transports as a function of the mean latitude suggests that there is no obvious relationship between the geostrophic transport (what is actually measured) and the latitude. Therefore, the long-term interannual variability (on the order of 0.4 PW peak to peak) is not convincingly driven by aliasing of the sections in space and is probably best described as ‘natural variability’.



Since the paper was published seven additional cruises were conducted. Currently, the container line that was used to conduct the XBT transects, altered there shipping route. Until a new ship company that operates between Cape Town (South Africa) and Buenos Aires (Argentina) can be find to conduct the cruises, the transects are conducted between Cape Town and Santos (Brazil).

The mean results of the 20 realizations are given in Table 1.

**Table 1.** Results for the total heat transport calculated by Garzoli and Baringer, (2007) (line 1), from the 3 transects conducted between Cape Town and Santos (line 2) and as an average of the 20 realizations (line 3).

<b>Mean Heat transport (14 realizations CT-BA) = 0.53 PW Std = <math>\pm 0.11</math> PW</b> <b>(Garzoli and Baringer, 2007)</b>	
<b>Mean Heat transport (3 transect CT-R) = 0.54 PW</b>	<b>Std= <math>\pm 0.10</math> PW.</b>
<b>Mean Heat transport (20 realizations) = 0.53 PW</b>	<b>Std = <math>\pm 0.12</math> PW</b>

The variability with time is shown in Figure 3. Different colors represents the different components of the heat transport: geostrophic, Ekman component and total heat transport, the later estimated as the sum of the previous two. The last 3 points (indicated as yellow) correspond to the last 3 cruises conducted along a slightly different route.

The total transport obtained from the last 3 realizations that follows a different route (0.54 PW) doer not differ significantly than the one obtained from the results from Garzoli and Baringer (14 realizations, 0.53 PW). The mean transport from the total 20 cruises is  $0.53 \pm 0.12$  PW.

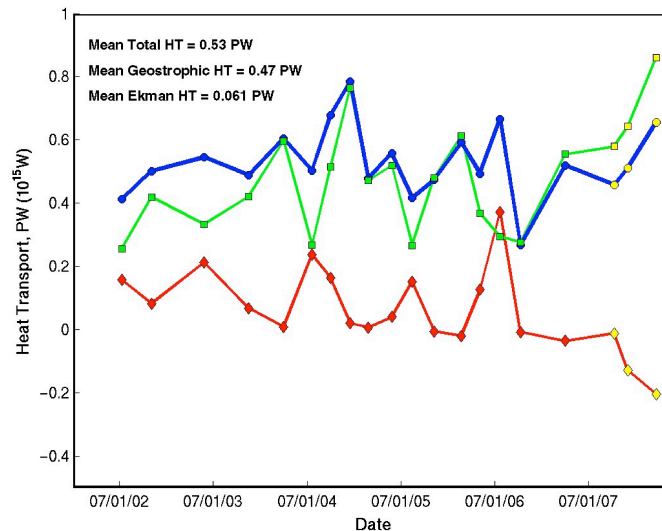


**Figure 3.** Variability with time of the total (blue), geostrophic (green) and Ekman (red) fluxes. The last three points corresponds to the route Cape Town to Santos.

It is interesting to note that at the end of the record (Figure 3) the geostrophic component has increased while the Ekman component decreased. As a result the total heat transport remains the same. To illustrate why this happens, Figure 4 shows the time series of the Ekman heat transport integrated across the basin as a function of latitude. Dots indicate mean latitude of each cruise. The last 3 cruises (Cape Town to Santos) were conducted at latitude located in the mean further north than the previous transects and in a region where during that time of the year (southern hemisphere summer) the Ekman fluxes are negative. Also during the southern hemisphere summer, the Brazil Current reached its southern-most extension.

As reported by Garzoli and Baringer (2007) the total heat transport shows apparent interannual variability, but does not show a strong indication of seasonality. However the Ekman and geostrophic components of the heat flux (Figure 5) show indications of an annual cycle that explains 80% of the total variance. The cycles are out of phase and therefore the total heat flux does not show any significant seasonality.

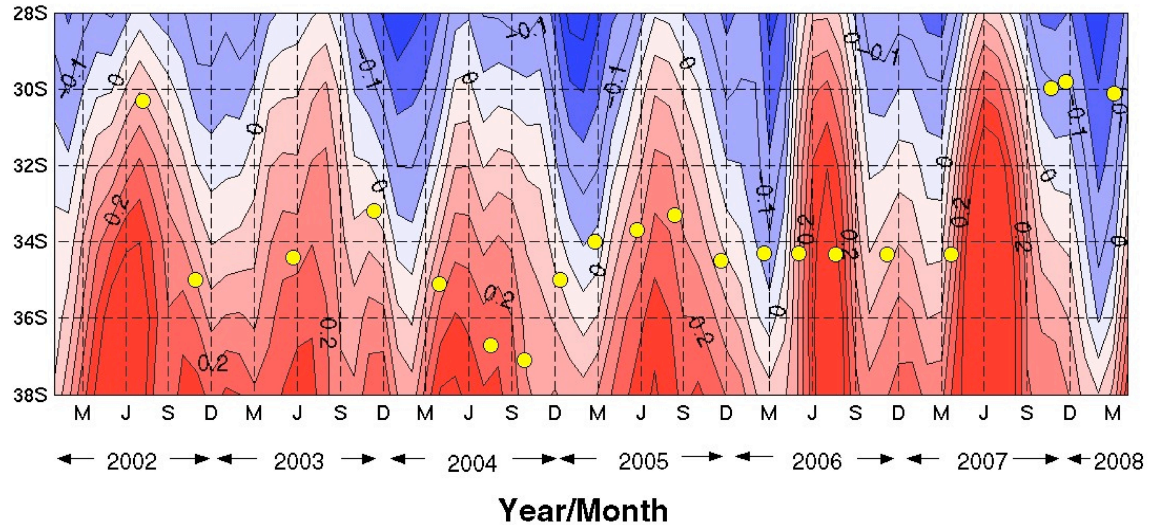


**Figure 4.** Time series of the Ekman Heat transport integrated across the basin as a function of latitude. Dots indicate mean latitude of each cruise.

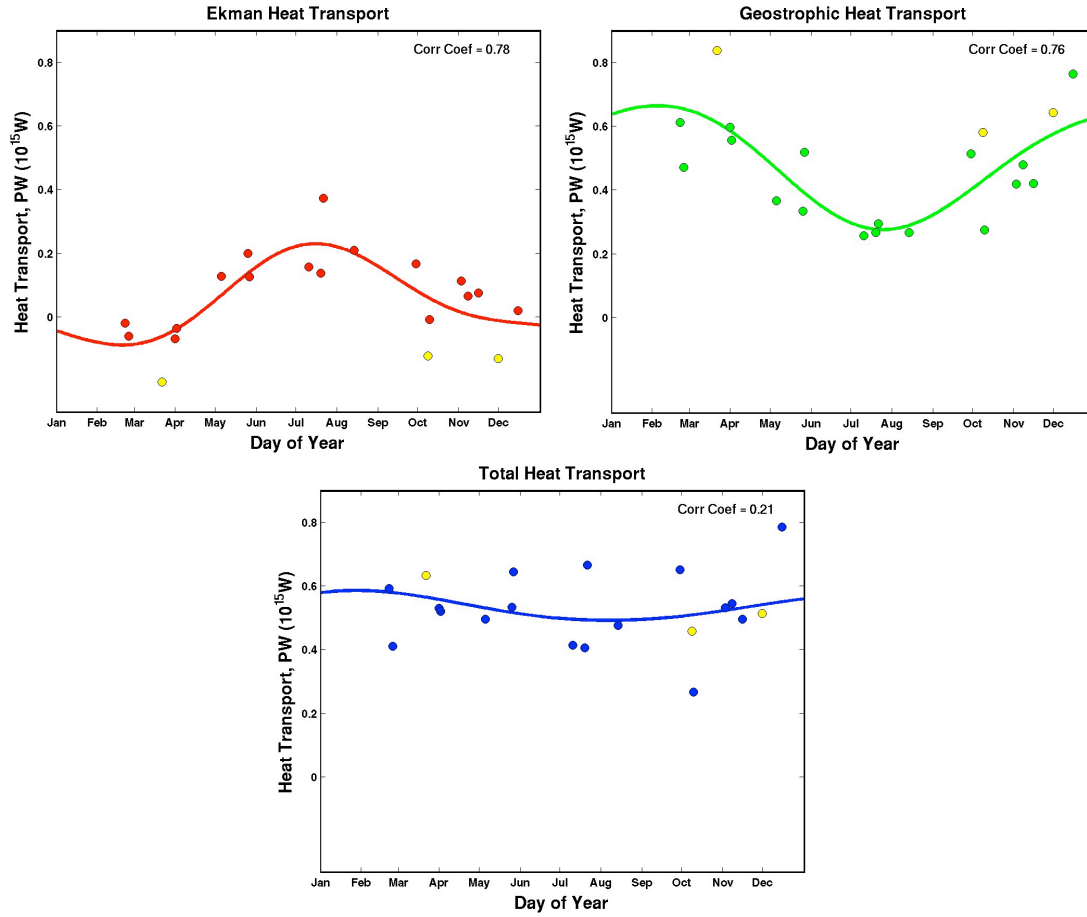


**Figure 5.** Annual cycle of Ekman and geostrophic components (top), and total heat transport (bottom) across the AX18 20 realizations. Results from the 3 lines occupied from Cape Town to Rio are shown in a different color (yellow).

### *North Atlantic:*

The heat transport was found to vary on inter-annual time scales from  $0.8 \pm 0.2$  PW at in 2003 to  $1.2 \pm 0.2$  PW in 1996 and the present with instantaneous estimates ranging from 0.6 to 1.6 PW (Figure 6 and Figure 1). Heat transport due to Ekman layer flow computed from annual Hellerman winds was relatively small (only 0.1 PW). This variability is entirely driven by changes in the interior density field; the barotropic Florida Current transport was kept fixed ( $32 \text{ Sv}^3$ ). At low frequencies, North Atlantic heat transport variations were found to correlate with the Atlantic Multidecadal Oscillation (AMO) as shown in Figure 6.

<sup>3</sup> Sv is a Sverdrup or  $10^6 \text{ m}^3/\text{s}$ , a unit commonly used for ocean volume transports.

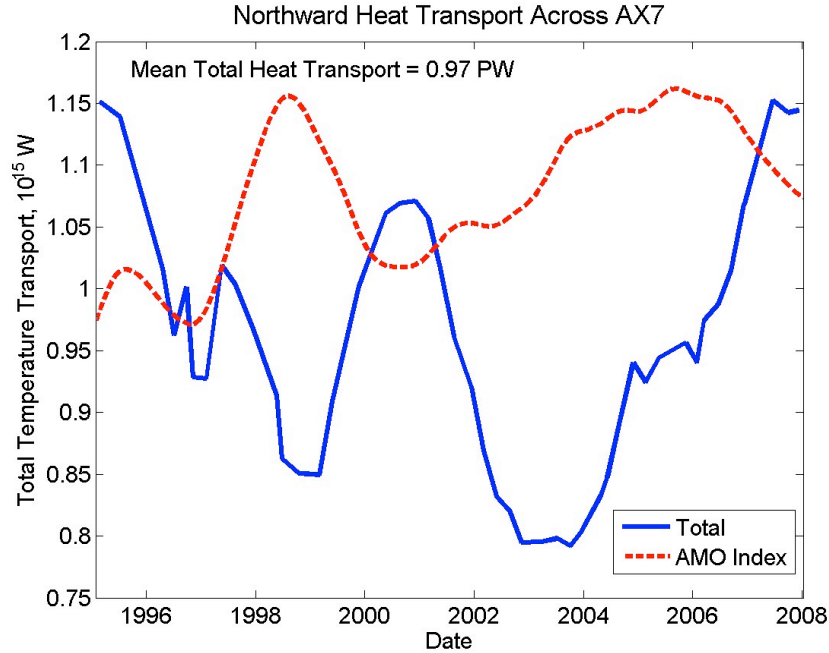


**Figure 6.** Time series of total heat transport in the center of the subtropical gyre in the North Atlantic Ocean along the XBT lined designated AX7. In the North Atlantic, there has been an oscillation in heat transport over the past 12 years (solid blue). The apparent trend through 2005 has ended with increasing northward heat transport in following years. Heat transport appears to be loosely inversely related to the Atlantic Multidecadal Oscillation (AMO) Index (red dashed).

### 2.3. Analysis of wind products

The heat transport is composed of two terms, the geostrophic component and the Ekman component, the last one estimated from wind products. As reported in the Plan for FY08, a comprehensive study of the wind products (climatology, reanalysis and satellite) was started to determine which is the most appropriate for each region and to estimate the errors incurred due to the use of different products. Up to date, the following was accomplished: The Ekman flux and the resulting total heat transport were obtained from three different wind products Hellerman, NCEP and ECMWF.

In the North Atlantic, Ekman heat flux (as opposed to temperature transport in the surface Ekman layer) is computed as the difference between the Ekman temperature transport in the surface mixed layer (defined using XBT observations for each month) and the mass-balancing transport of the vertically averaged ocean temperatures (defined as the areal averaged T from each XBT section). Results are shown in Figure 7. The Ekman fluxes differ by less that 0.03 PW, hence the Hellerman Ekman fluxes were used.

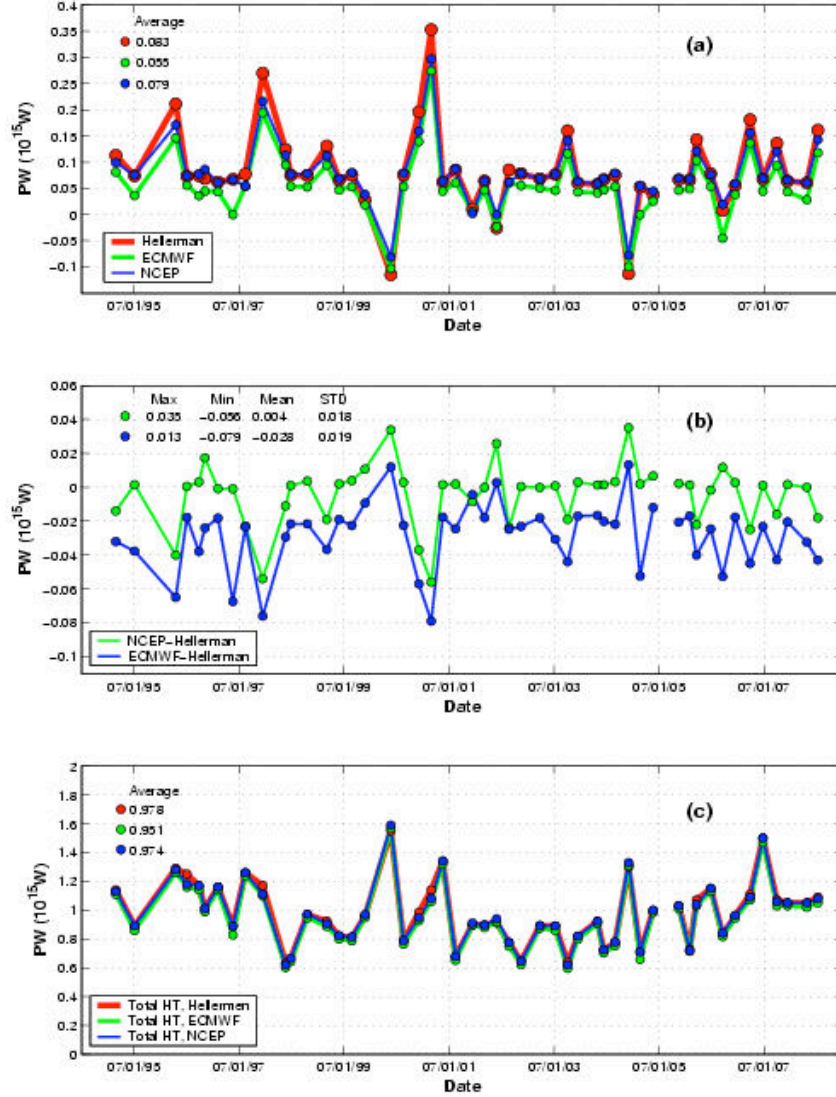


**Figure 7.** a) The Ekman flux is determined from the Hellerman annual mean climatology, the ECMWF monthly values and the NCEP monthly values. The Ekman fluxes differ by less than 0.03 PW. b) Differences between the Ekman fluxes above. The ECMWF fluxes are typically lower than the Hellerman or NCEP fluxes. c) The total heat transport using the three different Ekman flux estimates.

In the South Atlantic, the Ekman heat flux is computed as above: namely the total Ekman heat flux is defined as the difference between the Ekman temperature transport (in the Ekman layer) and the section average Temperature times the Ekman mass flux (so that the Ekman transport is mass-balanced). However several different areal Temperature averages were compared (defined as ‘cases’ below). Results are shown in Figure 8. The different average of total heat transport is less than 0.06 PW, however there are interesting variations over time linked to mesoscale variability in the region, Brazil Current meandering etc that the NCEP winds were used for the heat transport estimates.

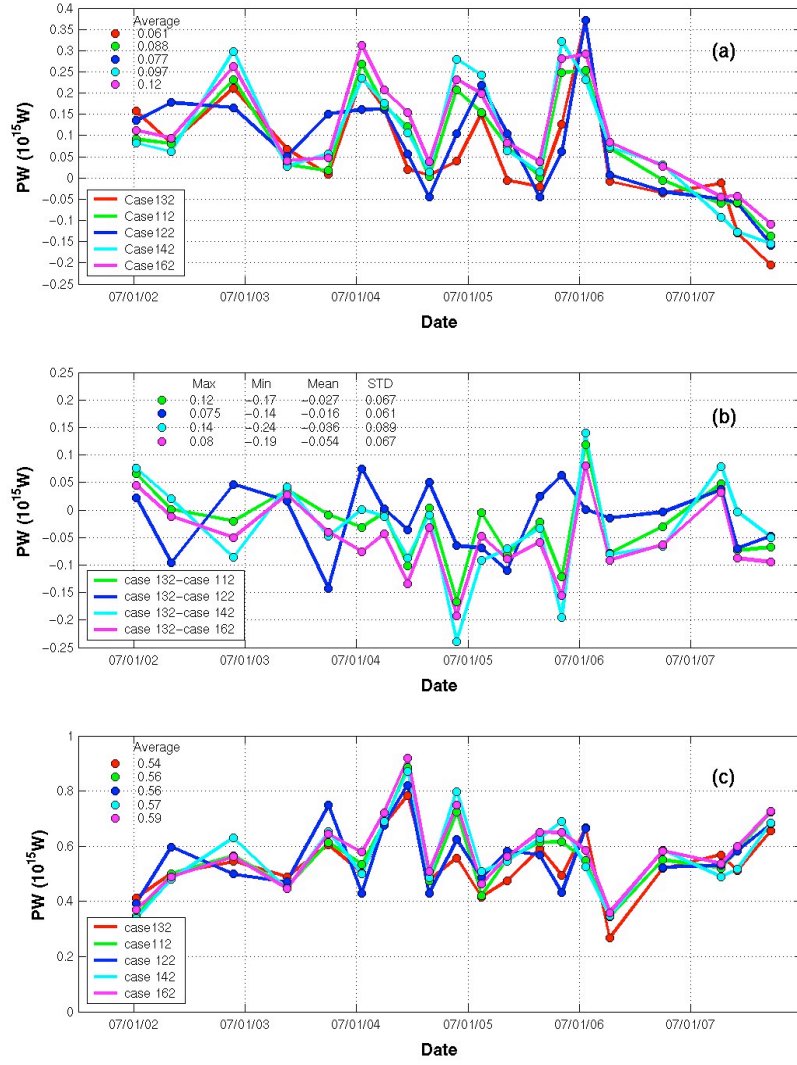


**Figure 8.** a) The Ekman flux is determined from wind stress values. The Ekman fluxes differ by less than 0.06 PW. b) Differences between the Ekman fluxes above. The case 132 fluxes are typically lower than other cases c) total heat transport using the five different Ekman flux estimates. ‘Cases’ are defined in Table 2.



**Table 2.** The Ekman heat fluxes shown in Figure 8 were computed from the ‘cases’ listed above. The temperature field used was either from the Levitus climatology alone or a combination of the XBT observations (0- 850 meters) and Levistu data (below 850 meters).

Case	Wind Product	Average Temperature from
case 132	NCEP monthly	Levitus temperature field.
case 112	NCEP monthly climatology	XBT-Levitus temperature field.
case 122	NCEP monthly	XBT-Levitus temperature field.
case 142	Hellerman annual mean	XBT-Levitus temperature field.
case 162	ECMWF monthly	XBT-Levitus temperature field.